Available online at www.sciencedirect.com
SCIENCE DIRECT®
Journal of Crystal Growth 274 (2005) 331–338
JOURNAL OF CRYSTAL GROWTH
www.elsevier.com/locate/jcrysgro

Comprehensive characterization of MOVPE-grown AlGaAs/AlAs distributed Bragg reflector structures by optical reflectance, X-ray diffraction and atomic force microscopy

A. Bhattacharya[a,*], M. Nasarek[b], U. Zeimer[b], A. Klein[b], M. Zorn[b], F. Bugge[b], S. Gramlich[b], M. Weyers[b]

[a]*Department of Condensed Matter Physics and Materials Science, Tata Institute of Fundamental Research, Mumbai, India*
[b]*Ferdinand-Braun-Institut für Höchstfrequenztechnik, Gustav-Kirchhoff-Str. 4, D-12489 Berlin, Germany*

Received 28 April 2004; accepted 7 October 2004
Communicated by T.F. Kuech
Available online 25 November 2004

Abstract

This paper reports on a comprehensive characterization of MOVPE-grown $Al_xGa_{1-x}As$/AlAs distributed Bragg reflector (DBR) structures via optical reflectance, X-ray diffraction (XRD) and atomic force microscopy (AFM). These analytical techniques are used to investigate the influence of parameters like substrate misorientation, aluminum content and number of mirror pairs on the characteristics of high-reflectivity $Al_xGa_{1-x}As$/AlAs-based Bragg mirrors. We find a strong correlation between the optical reflectivity of the DBR mirrors and the quality of X-ray rocking curves as well as the surface/interface roughness as measured by AFM. The data provided by these analytical techniques are used to optimize the DBR performance for its application in visible-wavelength vertical-cavity surface-emitting laser (VCSEL) diodes.

Keywords: A1. High resolution X-ray diffraction; A1. Interfaces; A1. Optical reflectivity; A3. Metalorganic vapor phase epitaxy; A3. Superlattices; B2. Semiconducting aluminium compounds

1. Introduction

Visible-wavelength vertical-cavity surface-emitting lasers VCSELs ($\lambda \sim 650$ nm) are ideal light sources for many emerging opto-electronic technologies such as plastic-fiber-based communication, high-density optical storage systems, and high-definition laser printing [1,2]. The VCSEL geometry with a short active region, typically one wavelength thick, results in a very small gain length and hence requires exceptionally high mirror reflectivities (>99.5%) surrounding the

*Corresponding author. Tel.: +91 22 22804545; fax: +91 22 22804610.
E-mail address: arnab@tifr.res.in (A. Bhattacharya).

0022-0248/$ - see front matter © 2004 Elsevier B.V. All rights reserved.
doi:10.1016/j.jcrysgro.2004.10.008

cavity to achieve a reasonable threshold current density. Such high reflectivities are usually provided by quarter-wave $Al_xGa_{1-x}As$/AlAs distributed Bragg reflector (DBR) mirrors. These mirrors must additionally be transparent at the operating wavelength. At $\lambda \sim 650$ nm an Al concentration of $x \geqslant 0.5$ is necessary in the high-index layer for low absorption thus reducing the index contrast ratio and requiring a large number of DBR periods to achieve the necessary high reflectivities. Visible VCSELs normally employ 50–55 pairs in the lower n:DBR and ~35 pairs in the upper p:DBR thus making the layer stack extremely thick (~8–9 μm) [3]. This raises particularly difficult growth issues as tight control over the layer thickness, composition and growth rate has to be maintained over a relatively long growth period [4]. This paper presents details on the influence of the substrate misorientation and the aluminium concentration on the characteristics of high-reflectivity $Al_xGa_{1-x}As$/AlAs-based Bragg mirrors.

2. Experimental details

All the DBR structures discussed in this work were grown in an Aixtron-200 low-pressure metal-organic vapor-phase epitaxy (MOVPE) system. The sources used were trimethylgallium (TMGa), trimethylaluminum (TMAl) and arsine (AsH_3). The growth pressure was 70 mbar and the growth temperature was set to 770 °C. Epi-ready n^+ GaAs substrates were used—both nominally exact[1] (0 0 1) on-axis oriented as well as wafers intentionally misoriented 6° toward ⟨1 1 1⟩A. The $Al_xGa_{1-x}As$ /AlAs DBR mirrors were grown without any interrupts at the interfaces with growth rates of ~10 Å/s for $Al_xGa_{1-x}As$ and ~5 Å/s for AlAs. This was found to result in the best structural quality as evidenced from the X-ray rocking curves. Typical layer thicknesses were 52 nm for the AlAs and 47 nm for the $Al_{0.6}Ga_{0.4}As$ layers. If not stated otherwise the Al content (x-value) was 0.6, apart from a series of experiments where it was varied from 0 to 0.6 to show the influence of the Al-concentration on the layer and interface quality. The number of $Al_xGa_{1-x}As$ /AlAs mirror pairs was varied from 10 to 40 for the structural experiments and was set to 50 for the n-side mirror and to 30 for the p-side mirror in the complete VCSEL structure.

Reflectance spectra for the DBR mirrors and VCSEL structures were measured in the 540–740 nm range relative to a standard dielectric mirror. A collimated beam from a white-light source was focussed onto the sample at normal incidence and the reflected light was imaged into a 0.32 m focal length monochromator. The measured absolute reflectivity was accurate to 0.5%, sufficient to quantify the relevant reflectance features like position and width of the high-reflectivity region across the wafer.

To extract structural information, the measured spectra were compared to simulated curves obtained using a transfer-matrix method [5,6] to calculate the reflectivity of a multilayer dielectric stack. The simulation program used [7] permits not only variations in the layer composition and thicknesses, but can also take into account parameters like energy-dependent absorption, thickness fluctuations and interface roughness. These simulations also helped us to identify the slope of the sidewalls of the central high-reflectivity plateau ($dR/d\lambda$) as a sensitive parameter in judging the structural perfection of the DBR from the reflectivity spectrum. For comparability $dR/d\lambda$ was always taken at half-maximum. For example, a random ±1% change around the target $\lambda/4$ layer thickness of the individual layers, or a 1% difference in layer thickness from bottom to top changes the peak reflectivity of a 30-pair DBR by only 0.001%–0.01%. However, the slope $dR/d\lambda$ of the central plateau is reduced by about 1% in either case, thus highlighting the sensitivity of this parameter in judging the quality of a DBR.

Structural characterization was also provided via high-resolution X-ray diffraction (XRD) rocking curves recorded using a Philips material research diffractometer with $CuK\alpha_1$ X-rays of <10 arc sec beam divergence in the scattering plane. $\Omega/2\Theta$-rocking curves were measured in both the (0 0 4) and the (0 0 2) reflections. As the atomic scattering factors for Ga and As almost

[1]The vendor specification for the possible miscut of the on axis (0 0 1) wafers is ±0.5°. This was verified using XRD.

cancel out in the (0 0 2) reflection, it is more sensitive to the scattering from the superlattice structure. The measured rocking curves were simulated using Philips EPITAXY^{TM} software based on dynamical XRD theory. Ideally, the same set of parameters would be expected to satisfy the (0 0 4) and the (0 0 2) scans. However, the (0 0 2) scans also penetrate deeper into the multilayer stack and hence, a discrepancy in the fitting parameters for the (0 0 2) and (0 0 4) scans can be used to investigate vertical inhomogeneities in thick superlattice structures.

The intensity and the full-width at half-maximum (FWHM) of the satellite peaks of a superlattice rocking curve can provide a quantitative estimate on inhomogeneity in the vertical periodicity [8]. First, the bending of the layer stack due to elastic deformation leads to a broadening of the substrate peak as well as of all satellite peaks. This effect can be considered in the simulations by fitting the substrate peak FWHM using a certain radius of curvature. Additionally, changes in periodicity cause a further broadening in the half-widths of the superlattice satellite peaks. In particular, for a statistical Gaussian distribution of period variations, the product of the intensity and half-width remains almost constant, and the period fluctuation ΔP can be estimated from $\Delta P/P \sim \Delta q/(q-q_B)$ where Δq is the half-width of a satellite, with q_B being the substrate peak position. This allows the separation of the two contributions to the satellite peak FWHM, i.e. bending and periodicity. In contrast, interfacial roughness alone, which does not affect the periodicity, has almost no influence on the half-width, but causes a reduction in intensity of the outer satellites due to enhanced diffuse scattering.

Surface roughness of the DBR structures was estimated from atomic force microscopy images obtained using a Digital Instruments Nanoscope II AFM operating in tapping mode. The RMS value for roughness evaluated over a $5 \times 5\,\mu m$ field was used in all cases. In order to measure the roughness of the interfaces *within* the DBR structures, the samples were ground and polished using diamond lapping film with 0.1 μm grain size at a bevelled angle of nearly 0.3°. As a result, the 50 nm thick layers were spread out to 10 μm at the surface of the bevelled sample. To remove the surface damage and to uncover the $Al_xGa_{1-x}As$ interfaces the sample surface was etched with 7.5% HF solution. The etch rate for AlAs in HF is almost an order of magnitude higher than for the $Al_xGa_{1-x}As$ layers. Thus, at the bevelled edge, the individual $Al_xGa_{1-x}As$ layers are exposed as terraces, thus enabling AFM observations to be carried out at various depths within the structure. This permits a post-growth study of the development of the surface roughness during the growth of the DBR stack. Such roughness measurements have been shown to correlate very well with the surface roughness that can be extracted from time-resolved in situ UV remeasurements of complete VCSEL structures [9].

3. Results and discussion

3.1. Optical characterization

The solid curve in Fig. 1 shows the calculated peak reflectivity as a function of the number of pairs for an $Al_{0.6}Ga_{0.4}As/AlAs$ DBR centered at $\lambda = 650$ nm. The reflectivity increases rapidly at first, and then slowly saturates with a 40-pair DBR having 99.9% reflectivity. The same figure also shows the measured peak reflectivity data for a

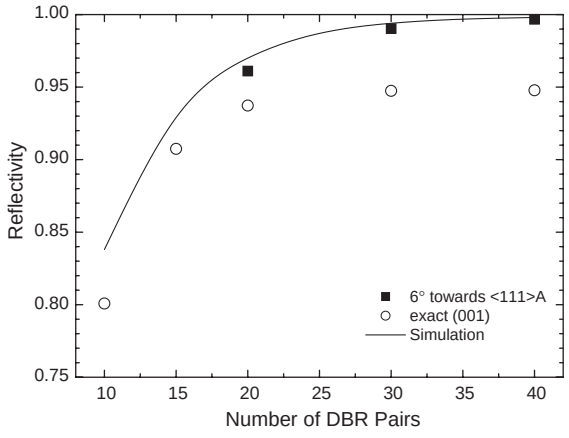

Fig. 1. Dependence of DBR reflectivity on number of $Al_{0.6}Ga_{0.4}As/AlAs$ pairs for exactly (0 0 1) oriented samples and samples misoriented 6° toward ⟨1 1 1⟩A. The calculated reflectivity is also shown for comparison.

series of $Al_{0.6}Ga_{0.4}As$/AlAs-based Bragg mirrors centered around the 650 nm wavelength region differing only in the number of mirror pairs but otherwise grown under identical conditions. DBRs grown on exactly (0 0 1) oriented substrates, which are typically used for $Al_xGa_{1-x}As$-based edge-emitting lasers, have reflectivity values much lower than the theoretically expected ones, and show a deterioration of mirror quality with increasing number of mirror pairs (open circles). The peak reflectivity is limited to ~95% even with 40-pair DBRs. Growth on substrates misoriented 6° toward ⟨1 1 1⟩A offer improved performance, with the measured reflectivity closer to the calculated values. (This is fortuitous, as the 6°-misoriented substrates are also better suited for the AlGaInP-based active region [10]).

In Fig. 2 the slope of the sidewall of the central high-reflectivity plateau ($dR/d\lambda$) at half-maximum is plotted as a function of the peak reflectivity while the inset shows a representative reflectance spectrum of a DBR mirror. The earlier section discussed the use of this parameter as a measure of perfection of the mirror stack. In spite of the higher measured reflectivities of DBRs grown on the misoriented substrates the $dR/d\lambda$ values are still below the expected values, suggesting layer thickness variation, interfacial roughness and/or other causes for deterioration in the DBR perfection.

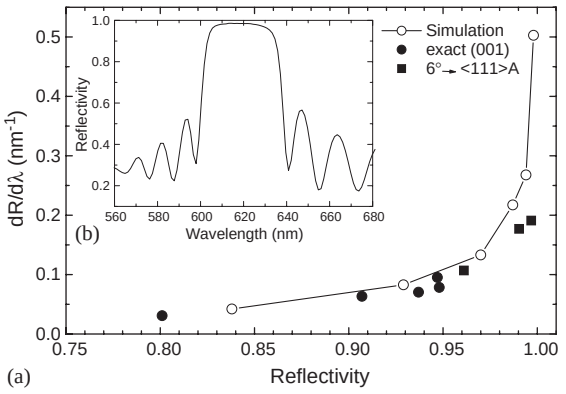

Fig. 2. Dependence of $dR/d\lambda$, the slope of the central high reflectivity plateau at half-maximum, on peak reflectivity for exact (0 0 1) oriented samples and samples misoriented 6° toward ⟨1 1 1⟩A shown in Fig. 1. The solid line plots the ideal $dR/d\lambda$ value. Inset: Representative reflectance spectrum of a DBR mirror.

3.2. X-ray characterization

High-resolution X-ray rocking curves have been measured both for the (0 0 4) and (0 0 2) reflections. Since in all the cases we were able to fit the curves by simulations using the same parameter set for both reflections we conclude that there are no gradients in the vertical periodicity of the layer stack, i.e. periodicity fluctuations do not vary from bottom to top. The bending of the layer stack due to elastic strain was considered by fitting the half-width of the substrate peak and introducing a certain radius of curvature into the simulations. Since the introduction of the radius of curvature leads to a broadening of the half-widths of all satellite peaks in the same way a broadening beyond this can be ascribed to periodicity fluctuations.

X-ray rocking curves of the DBRs grown on exactly (0 0 1) oriented substrates and substrates misoriented 6° toward ⟨1 1 1⟩A exhibit considerable differences. Fig. 3 shows the (0 0 2) rocking curves of 30-pair $Al_{0.6}Ga_{0.4}As$/AlAs DBRs whose reflectivity data were presented in the previous section. It can clearly be seen that the satellite peaks in the exact-substrate case are considerably

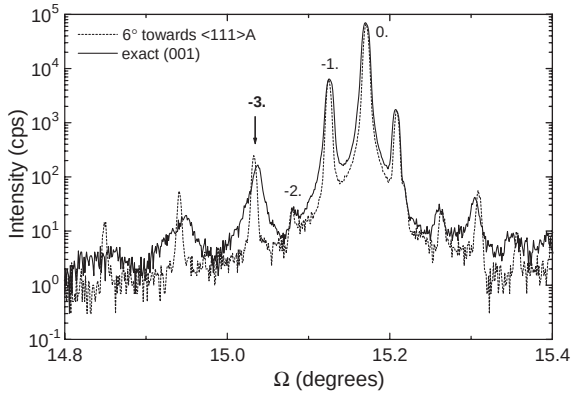

Fig. 3. X-ray rocking curves in the (0 0 2) reflection for 30-pair $Al_{0.6}Ga_{0.4}As$/AlAs DBRs grown on exact (0 0 1) oriented samples and samples misoriented 6° toward ⟨1 1 1⟩A. The arrow indicates the third satellite on the left of the zero order peak.

broader and less intense than in the sample misoriented 6° toward ⟨1 1 1⟩A. Also, a lesser number of satellite peaks can be distinguished in the exact (0 0 1) case. To study this trend further, in Fig. 4 we track the half-width (a) and intensity (b) of an arbitrary, fixed satellite peak, namely the third satellite on the left of the 0th order peak, (arrow in the figure) versus the number of mirror pairs. The values expected for an ideal DBR based on dynamical diffraction theory are also plotted. We observe a sharp *rise* in the satellite half-widths for thick DBRs in both the exact and misoriented cases, with the latter having narrower peak widths for all the samples. The peak intensity remains almost constant for the exact substrate and actually decreases with increasing DBR thickness for the misoriented case. Both these observations are in sharp contrast to the theoretical expectations and strongly point to significant degradation in structural perfection of the superlattice. Using the rocking curves in Fig. 3 along with the equation discussed in the preceding section to estimate the period fluctuation leads to a value of ~7 nm for the exact (0 0 1) and ~2 nm for the 6°-misoriented cases.

It is interesting to compare X-ray rocking curves of superlattices of varying Al composition. Fig. 5 plots the (0 0 2) rocking curves for 20-pair $Al_xGa_{1-x}As$/AlAs superlattices grown on exactly (0 0 1) oriented substrates with (a) $x=0$, (b) $x=0.25$, and (c) $x=0.6$. It is evident that the number of satellites visible decreases as the total Al content of the stack increases. This is accompanied by a broadening of the satellite peaks and a sharp drop in their intensity. $Al_xGa_{1-x}As$ is known to be more immune against plastic strain relaxation than theoretically predicted. Misfit dislocation formation was not observed in samples investigated using transmission electron microscopy (TEM)

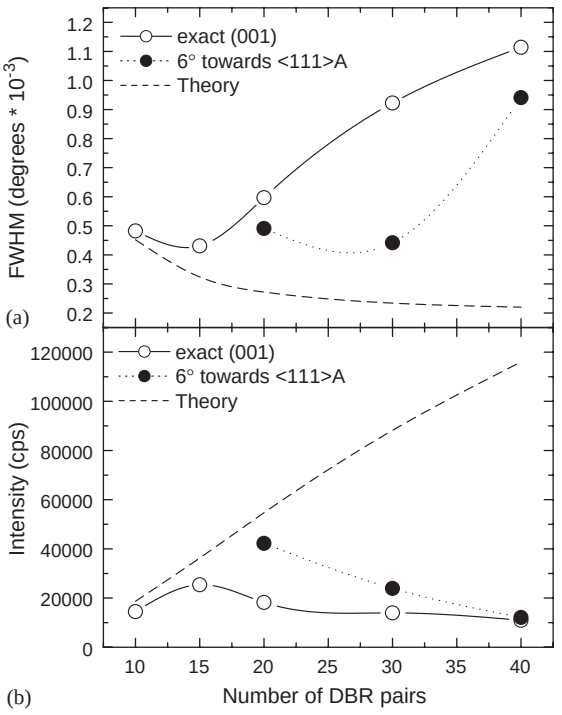

Fig. 4. The FWHM (a) and intensity (b) of the third satellite peak in the diffraction pattern versus the number of mirror pairs for DBRs grown on exact (0 0 1) oriented substrates and substrates misoriented 6° toward ⟨1 1 1⟩A. The thin lines are the trends expected from dynamical diffraction theory.

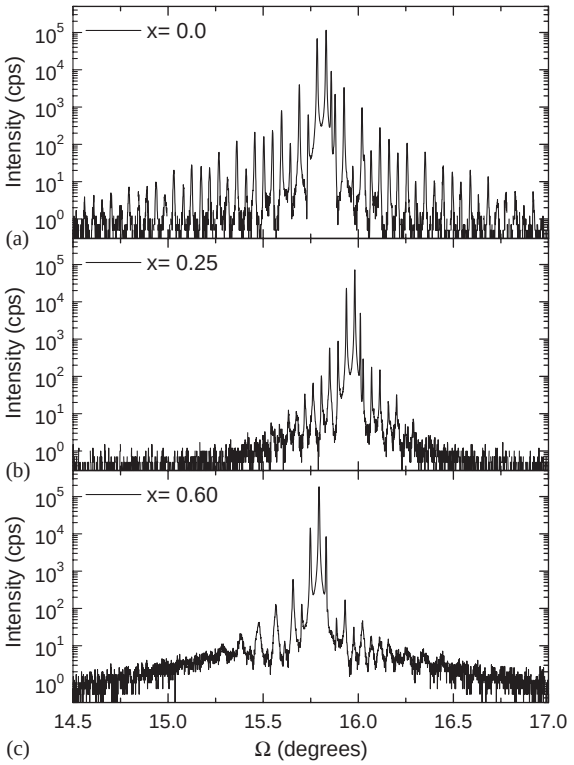

Fig. 5. (0 0 2) rocking curves for 20-pair $Al_xGa_{1-x}As$/AlAs superlattices with (a) $x=0$, (b) $x=0.25$ and (c) $x=0.6$ grown on exact (0 0 1) oriented substrates.

and no evidence of relaxation was found from the in-plane lattice parameter measured using asymmetric X-ray reflections. Nevertheless, the accumulated strain causes an increase of periodicity fluctuations and interface roughness during growth.

We have additionally verified via TEM that within the DBR stack the surfaces of the $Al_xGa_{1-x}As$ layers are indeed rougher than the surface of the next AlAs layer. The growth of the binary layer results in a smoother surface than the growth of the ternary one [11]. This would also explain the observation that the rocking curves of binary/binary GaAs/AlAs DBRs are almost close to that expected from theory. In contrast, in the case of a ternary/binary combination like $Al_xGa_{1-x}As$/AlAs, the rougher surface of the ternary layer leads to a lower intensity of the outer satellites in the diffraction pattern.

3.3. AFM characterization

Further evidence of a correlation between the surface roughness and the X-ray and optical properties comes from a direct observation of the DBR surface via atomic force microscopy. Fig. 6 plots the RMS values of surface roughness for the series of $Al_{0.6}Ga_{0.4}As$/AlAs mirrors described in the earlier sections for (a) exact oriented samples, and (b) samples misoriented 6° toward ⟨1 1 1⟩A. The insets show the AFM pictures for the 30-pair case. The same figures also include the X-ray FWHM data of Fig. 4 for comparison; the similarity in the two trends is obvious. An analysis of the data provides a value of 9.7 nm for the RMS roughness of the on-axis sample (a), and 1.2 nm for the sample misoriented 6° toward ⟨1 1 1⟩A (b). It is worth pointing out that the estimates from the rocking curves in Fig. 3 (7 and 2 nm, respectively) are pretty close to the measured RMS roughness values. Since the surface roughnesses of both the exact (0 0 1) oriented and the misoriented 6° toward ⟨1 1 1⟩A substrates do not differ, the observed differences in roughness of the DBRs are connected with the growth mechanism. The 6° off-oriented wafers offer more terraces with a closer spacing, i.e. more nucleation sites, for the layer-by-

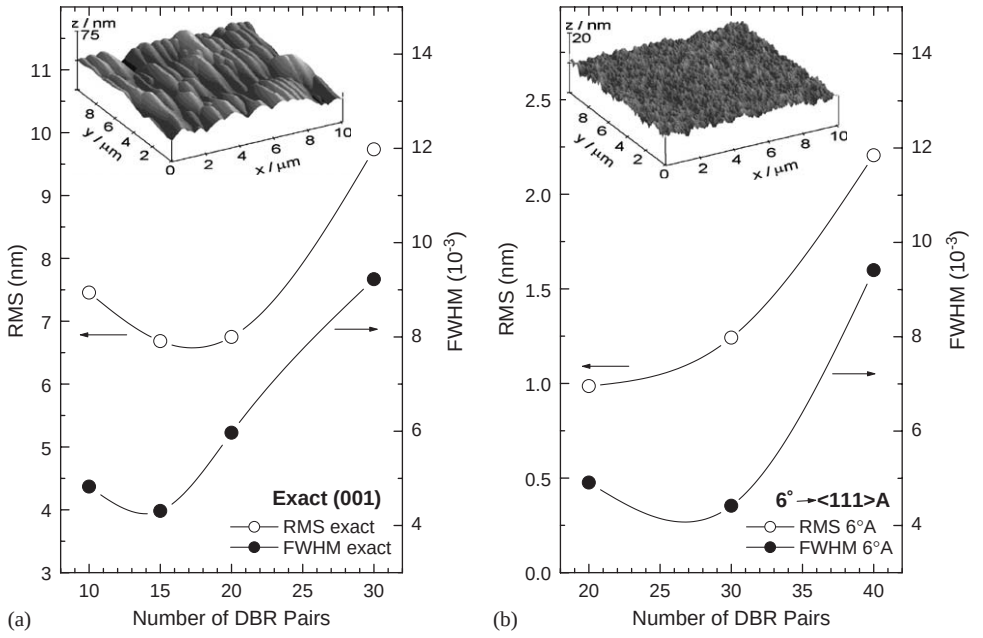

Fig. 6. RMS values of surface roughness for the series of $Al_{0.6}Ga_{0.4}As$ /AlAs mirrors for (a) exact (0 0 1) oriented samples and (b) for substrates misoriented 6° toward ⟨1 1 1⟩A. The trends in the X-ray half-widths from Fig. 4 are also included for comparison. The inset shows AFM pictures (scan size $10 \times 10\,\mu m^2$) of the surface of 30-pair $Al_{0.6}Ga_{0.4}As$/AlAs DBRs grown on (a) exact (0 0 1) oriented and (b) substrates misoriented 6° toward ⟨1 1 1⟩.

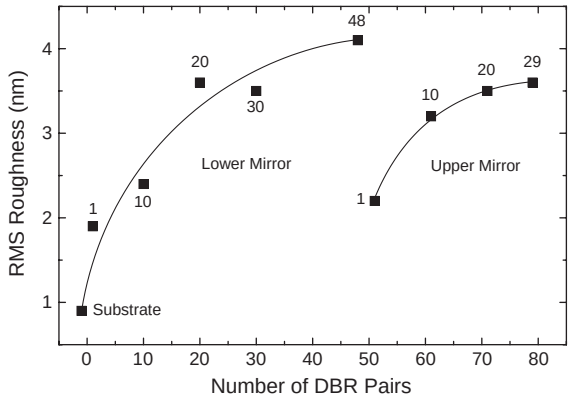

Fig. 7. RMS roughness at various depths *inside* a complete VCSEL structure.

layer growth. This apparently reduces the tendency for dynamic roughening observed on the exact (0 0 1) substrates.

In order to measure the roughness of the interfaces within the DBR structures, and thus investigate the development of the surface roughness during the growth of thick mirror stacks, complete VCSEL structures were etched with HF, exposing the constituent $Al_{0.6}Ga_{0.4}As$ layers as discussed earlier. Fig. 7 shows the RMS roughness at various depths *inside* a VCSEL structure consisting of a one wavelength thick (~185 nm) cavity sandwiched between a 50-pair lower n-DBR and a 30-pair upper p-DBR grown on a substrate misoriented 6° toward ⟨1 1 1⟩A. The numbers next to the data points indicate the position of the layer within the mirror. It is seen that the interface roughness gradually builds up during the growth, starting from a value of about 1 nm at the substrate and increasing to ~4 nm after 48 mirror pairs. It is striking that the growth of the AlGaInP cavity smoothens the surface remarkably, leaving an RMS roughness of ~2 nm at the beginning of the second DBR mirror. The growth of the second mirror again causes the interface roughness to increase to a value of about 3.5 nm after 30 pairs. The final roughness is thus almost the same as the roughness of the n:DBR at the 30-pair stage. A complete discussion of surface roughness within VCSEL structures including the differences in the n- and p-DBRs and the effect of the AlGaInP cavity has been presented in Ref. [9].

4. Summary

We have presented a detailed study of optical and structural characterization of $Al_xGa_{1-x}As$/AlAs DBR mirror stacks. While DBR mirrors grown on substrates misoriented 6° toward ⟨1 1 1⟩A offer much better reflectance than corresponding structures grown on exactly (0 0 1) oriented substrates, the structural perfection of the superlattice assessed by optical as well as X-ray techniques is still far from that expected theoretically. In the reflectivity spectrum the slope of the sidewall of the central high-reflectivity plateau at half-maximum, $dR/d\lambda$, is found to be smaller than in the ideal case. X-ray rocking curves show satellite peaks which are broader and less intense than predicted. These findings are correlated to the roughness of the layers measured via atomic force microscopy. Such a comprehensive characterization of the DBR mirrors is invaluable in optimizing the structures for state-of-the-art visible VCSEL devices [12].

Acknowledgments

The authors thank O. Fink for technical assistance at the MOVPE system. One of the authors (AB) is grateful for the support of the Ferdinand-Braun-Institut-Berlin where the experimental work was carried out under a research fellowship from the Alexander-von-Humboldt foundation.

References

[1] W.W. Chow, K.D. Choquette, M.H. Crawford, K.L. Lear, G.R. Hadley, IEEE J. Quant. Electron. QE-33 (1997) 1810.
[2] R.P. Schneider Jr., J.A. Lott, K.L. Lear, K.D. Choquette, M.H. Crawford, S.P. Kilcoyne, J.J. Fiegel, J. Crystal Growth 145 (1994) 838.
[3] M. Zorn, A. Knigge, U. Zeimer, A. Klein, H. Kissel, M. Weyers, G. Tränkle, J. Crystal Growth 248 (2003) 186.

[4] M. Zorn, K. Haberland, A. Knigge, A. Bhattacharya, M. Weyers, J.-T. Zettler, W. Richter, J. Crystal Growth 235 (2002) 25.
[5] F. Abelès, Ann. de Physique, 5 (1950) 596 and 706.
[6] M. Born, E. Wolf, Principles of Optics, Pergamon Press, Oxford, 1987.
[7] M. Nasarek, Charakterisierung von AlGaAs/AlAs Bragg-Spiegeln für die Optimierung von oberflächenemittierenden Lasern ($\lambda \sim 650$ nm), Diploma Thesis, Humboldt University, Berlin, 2000.
[8] D.K. Bowen, B.K. Tanner, High Resolution X-ray Diffractometry and Topography, Taylor & Francis Ltd., London, 1998, pp. 141–148.
[9] K. Haberland, M. Zorn, A. Klein, A. Bhattacharya, M. Weyers, J.-T. Zettler, W. Richter, J. Crystal Growth 248 (2003) 194.
[10] R.P. Schneider Jr., R.P. Bryan, J.A. Lott, E.D. Jones, G.R. Olbright, J. Crystal Growth 124 (1992) 763.
[11] S.F. Yoon, J. Electron. Eng. 13 (1993) 10.
[12] A. Knigge, M. Zorn, M. Weyers, G. Tränkle, Electron. Lett. 38 (2002) 882.